

Optogenetic Inactivation Modifies Monkey Visuomotor Behavior

James Cavanaugh,^{1,4,*} Ilya E. Monosov,^{1,4} Kerry McAlonan,¹ Rebecca Berman,¹ Mitchell K. Smith,¹ Vania Cao,² Kuan H. Wang,² Edward S. Boyden,³ and Robert H. Wurtz¹

¹Laboratory of Sensorimotor Research, National Eye Institute, NIH, Bethesda, MD 20982-4435, USA

²Unit on Neural Circuits and Adaptive Behaviors, Genes Cognition and Psychosis Program, National Institute of Mental Health, NIH, Bethesda, MD 20892, USA

³Department of Biological Engineering and Brain and Cognitive Sciences, MIT, Cambridge, MA 02139, USA

⁴These authors contributed equally to this work

*Correspondence: jrc@lsr.nei.nih.gov

<http://dx.doi.org/10.1016/j.neuron.2012.10.016>

SUMMARY

A critical technique for understanding how neuronal activity contributes to behavior is determining whether perturbing it changes behavior. The advent of optogenetic techniques allows the immediately reversible alteration of neuronal activity in contrast to chemical approaches lasting minutes to hours. Modification of behavior using optogenetics has had substantial success in rodents but has not been as successful in monkeys. Here, we show how optogenetic inactivation of superior colliculus neurons in awake monkeys leads to clear and repeatable behavioral deficits in the metrics of saccadic eye movements. We used our observations to evaluate principles governing the use of optogenetic techniques in the study of the neuronal bases of behavior in monkeys, particularly how experimental design must address relevant parameters, such as the application of light to subcortical structures, the spread of viral injections, and the extent of neuronal inactivation with light.

INTRODUCTION

A major goal of systems neuroscience is to identify brain mechanisms responsible for specific behaviors. Correlation of neuronal activity to behavior led the way to the identification of neuronal circuits underlying a wide range of sensory, motor, and cognitive behaviors in the primate model of human behavior. But linking neuronal activity to behavior requires another step: showing that modifying neuronal activity actually changes behavior.

Localized and reversible chemical inactivation of neurons is now widely used as a key test of which neuronal circuits underlie specific behaviors. Inactivation with anesthetics (such as lidocaine) or inhibitory transmitter agonists (such as muscimol) have been particularly useful because such inactivations last minutes to hours, so the activity of the brain during inactivation

can be tested before behavioral adaptation to the resulting deficit occurs. A substantial limitation of chemical inactivation, however, is that the effects persist until the drug is metabolized, and comparing its effects to a control condition on a trial-by-trial basis is impossible.

The recent introduction of optogenetic tools offers solutions to these limitations. Genetically encoded molecules target specific neurons in the brain, and enable their activity to be modulated by light. Optogenetic inactivation (as well as activation), developed primarily in rodents, has been effective in modifying behavior in vivo as shown in many studies (Knöpfel and Boyden, 2012; Tye and Deisseroth, 2012). Optogenetic techniques have also been implemented in monkeys, and the effectiveness of these techniques in turning on or off neurons has been amply demonstrated (Diester et al., 2011; Han et al., 2011; Han et al., 2009). However, experimentally changing monkey behavior by optogenetic techniques has remained elusive. Diester et al. (2011) tried to modify skeletal motor behavior by stimulating motor and somatosensory cortex of macaque monkeys using channel rhodopsin but found neither modulation of spontaneous activity of the resting arm and hand, nor an effect of optical stimulation with simultaneous electrical stimulation of motor and somatosensory cortex.

We reasoned that a more sensitive measure of behavior might show effects of optogenetic manipulation. We decided to determine if optogenetic manipulation of neurons within the superior colliculus (SC) could influence visually guided saccadic eye movements, which can be measured with great precision. Neurons at a given location in the intermediate layers of the SC discharge before saccades to a given region of the visual field, and their chemical inactivation alters the endpoint, velocity, and latency of these saccades. Furthermore, these neurons are organized into a precise representation of the visual field (Robinson, 1972), so we can predict exactly where in the visual field changes in neuronal activity should produce changes in behavior. We therefore introduced the light-driven outward proton pump ArchT (Chow et al., 2010; Han et al., 2011) into SC intermediate layer neurons. We found that optogenetically inactivating these SC neurons produced clear and repeatable deficits in saccades. We have used these deficits along with the SC map to explore the advantages and limitations of optogenetic modulation of monkey behavior.

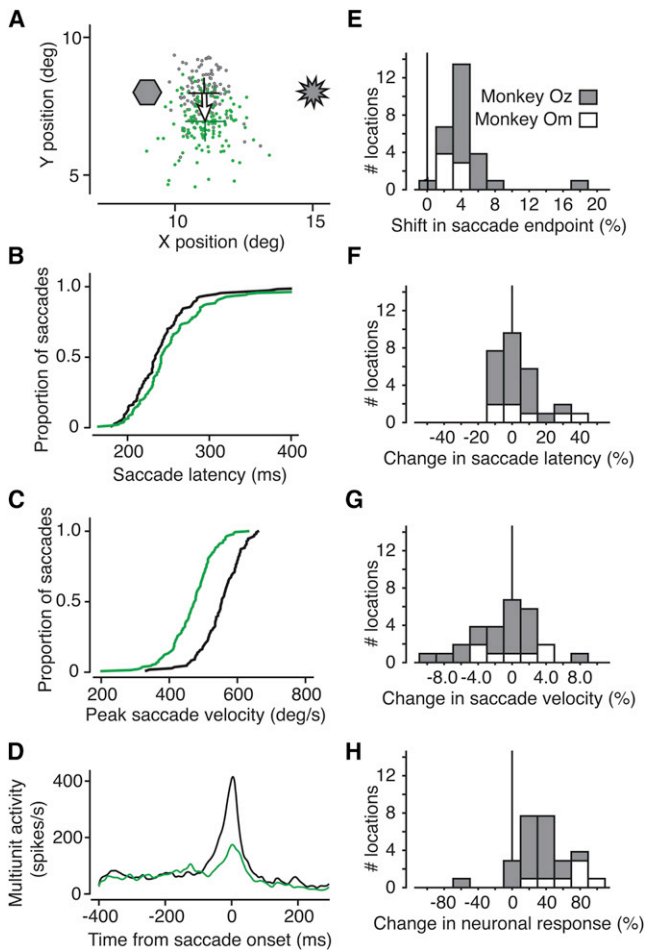


Figure 1. Behavioral Effects from Optogenetic Control

(A) Saccades with and without laser stimulation directed to a visual target at 11.5° , 8.0° . Saccade endpoints are shown without (gray) and with (green) laser stimulation. Laser light was introduced into the intermediate layers of the SC on randomly interleaved trials. This was done by opening and closing a fast shutter placed in the path of the laser, which remained on throughout the experiment. Green and black crosses indicate the mean saccade endpoints (± 1 SEM) with and without light, respectively. This example was chosen as a clear demonstration, but most results were based on fewer trials. (B) Cumulative distribution of saccade latencies for this example. Black are latencies without light, green are in the presence of laser light. (C) Cumulative distributions of peak saccade velocity. The green trace shows peak velocity in the presence of laser light, and the black trace is without light. (D) Multiunit neuronal activity with and without laser stimulation for this example. Neuronal responses are shown as spike density histograms aligned to saccade onset at time zero and smoothed with a Gaussian filter with a 5 ms SD. Changes in neuronal activity were not related to shifts in saccade endpoint (see Figure S1). (E–H) Distributions of these effects for 28 experiments in two monkeys.

RESULTS

We studied optogenetic inactivation of one side of the SC in three monkeys. We injected an adenoassociated virus (AAV) incorporating ArchT fused to GFP (Han et al., 2011) and expressed under a pancellular promoter (CAG), into the intermediate layers of the SC. Neurons in these layers discharge before

saccades and their chemical inactivation produces deficits in saccades. At least 6 weeks after the injection of the virus, we tested the effect of shining green laser light (532 nm wavelength) onto these SC neurons. In two monkeys (OZ and OM), we presented the laser light while the monkey made visually guided saccades. In the third monkey (RO), we studied changes in neuronal responses during free viewing. The light reached the SC typically via a 200 μm diameter optic fiber attached to a recording electrode extending 500 μm beyond the flat fiber end (the optrode).

Modification of Saccadic Behavior

We found consistent behavioral effects in monkeys OZ and OM using laser light inactivation. Visually guided saccades showed the same triad of effects as with chemical inactivation: shift in saccadic end point, reduced peak velocity, and increased latency. Figure 1 shows the effects of laser inactivation at an example site in monkey OZ. We located the optrode in the SC intermediate layers during each experiment by the center of the movement fields represented by neuronal activity recorded 500 μm below the fiber tip. While the monkey fixated a central bright spot on a dark background, we presented a second spot of light and the monkey was rewarded for making a visually guided saccade to that spot once the fixation spot disappeared.

Figure 1A shows the locations in the visual field of the ArchT injection site (hexagon) and the optrode (starburst). Gray points are the endpoints of normal saccades to the visual target. Green points are saccade endpoints to the same visual target during SC inactivation. Saccade endpoints shifted on average about 1.02° down in this example (shown by the arrow), or about 7.3% of the saccade magnitude. These distributions of saccade endpoints were significantly different with and without light (2D Kolmogorov-Smirnov [KS] test, $p < 0.001$).

We did not methodically study the effect of laser intensity on behavior. However, we were of course able to eliminate any change in behavior by sufficiently turning down the laser from our default intensity of about 650 mW/mm^2 . Effects at less than 300 mW/mm^2 were negligible if present at all. Also, at several stimulation sites where we tested multiple laser intensities, we could not further increase the magnitude of the saccadic shift by increasing laser illumination, even up to 1600 mW/mm^2 .

In addition to changing the endpoints of saccades, photostimulation changed saccade latency and peak velocity. Figure 1B shows the cumulative distribution of saccade latencies without (black) and with (green) laser light. The distribution was shifted to the right with light, an increase of about 7 ms in saccade latency ($p = 0.020$, Wilcoxon rank-sum test). Figure 1C shows that the light shifted the distribution of peak saccade velocities to the left, a significant reduction in peak velocity of about $79^\circ/\text{s}$ ($p < 0.001$, t test). Note that subsequent p values without a specified test were obtained from a t test.

Figure 1D shows neuronal activity as spike density histograms, aligned to saccade onset. At this optrode location in the SC, multiunit activity representing the burst before the saccade decreased more than 60% with laser illumination, indicating a clear neuronal correlate for the behavioral changes we observed in saccade endpoint, saccade velocity, and saccade latency.

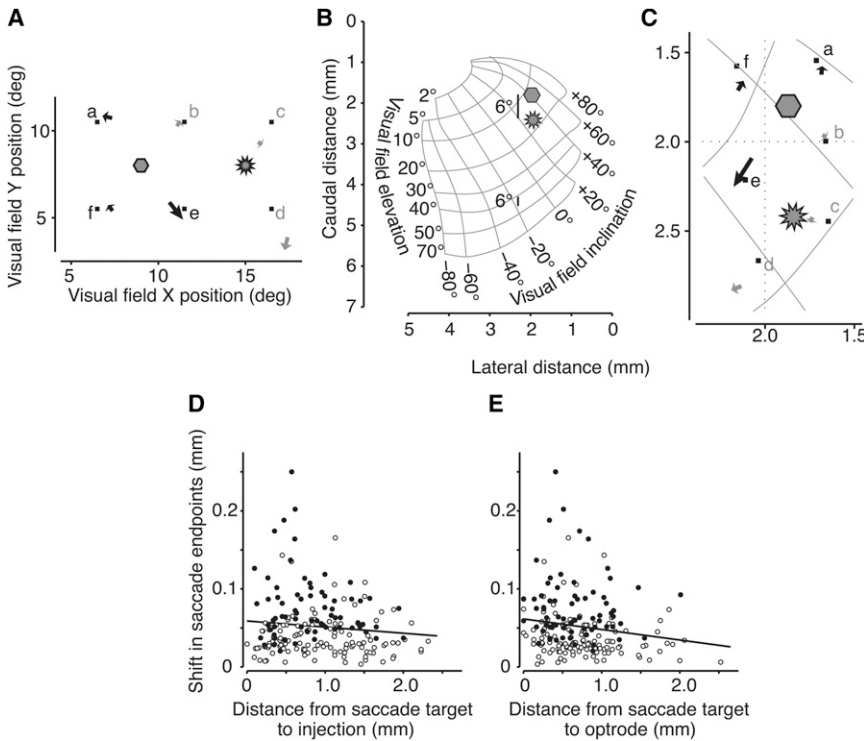


Figure 2. Magnitude of Saccadic Shift Diminishes with Distance from Both Injection and Laser Illumination

(A) Locations of the six targets in the visual field (small squares) along with the location of the injection site and the optrode site. Arrows show the shift in mean saccade endpoint when the SC was exposed to light. Significant shifts are plotted in black (gray otherwise). (B) Location on the collicular map of the injection (hexagon) and optrode (starburst) from the locations in (A). Bars subtending 6° of visual angle are shown for central and peripheral visual field locations to illustrate magnification within the SC map. (C) Region of interest on the SC map showing the injection, optrode, saccade targets, and shifts in saccade endpoints. Significant shifts are shown in black, gray otherwise. (D) Shift magnitude plotted against distance from injection. Both quantities are expressed as mm in the SC. Solid points denote significant shifts, whereas open symbols are not significant. The solid black line is the least-squares linear fit to all the data. (E) Shift magnitude plotted against distance from optrode. Symbols are the same as in (D).

Figures 1E–1H show the distributions of the above effects for 28 experiments. For the 21 experiments in OZ and the 7 in OM, the only difference between the monkeys was the reduction in neuronal response (most likely due to the fact that responses in monkey OM were recorded from single units, whereas in monkey OZ we predominantly recorded multiunit activity). For monkey OM, neuronal responses were reduced 68.2% on average ($p < 0.001$) and in monkey OZ 27.4% ($p < 0.001$). Saccade endpoints shifted an average of 4.6% of the saccade magnitude ($p < 0.001$, 2D KS test), latency increased 7.3 ms ($p = 0.20$, rank-sum test), and saccade velocity was reduced by $9.6^\circ/\text{s}$ ($p = 0.29$). As expected, there was no relationship between the changes in neuronal activity and changes in saccade endpoint (see Figure S1 available online).

In summary, we show that optogenetic inactivation of a region of the SC produced changes in saccades made to targets in the visual field near that same SC region. The shift in saccade endpoint and the changes in saccade peak velocity and latency were consistent with the deficits found with chemical inactivation (Hikosaka and Wurtz, 1985, 1986).

Relating the Magnitude of Shifts in Saccade Endpoint to Injection and Optrode Locations

A major advantage of testing optogenetic techniques in the monkey SC is that the locations of certain variables of interest, namely the shift in saccade endpoint, the location of the injection and the location of the optrode can all be represented on the same retinotopic map. This allows us to quantitatively evaluate how the spatial separation between the injection, the laser, and the active neurons affects the strength of optogenetic manipulations.

We presented saccade targets to monkey OZ at different locations in the visual field on randomly interleaved trials while the location of the injection and the optrode remained constant during an experiment. Figure 2 shows results from such an experiment (same optrode site as in Figure 1). On each trial we presented one of several targets, in this case six, distributed around both the injection site and the optrode site (Figure 2A). As before, the arrows show how the endpoints of saccades to each target shifted with light inactivation. Black arrows denote significant shifts, and gray arrows show those not reaching significance (2D KS test, $p < 0.01$). Changes in the saccade endpoints varied among targets in both direction and magnitude of the shift.

The first question is whether the magnitude of the behavioral effect (the shift in saccade endpoint) had any relation to the saccade target's distance from either the injection site or the optrode. The proper frame of reference to answer such questions is in the SC because the injection, the laser light, and the active neurons are each defined within the SC rather than the visual field, which is distorted by a magnification factor. This can be seen in Figure 2B which shows how 6° in the visual field (the distance between the injection site and this optrode site) subtends different distances on the SC depending on eccentricity. Also shown in Figure 2B are the same locations of the injection and optrode from Figure 2A on the SC map of the visual field. We have enlarged this region in Figure 2C to include the locations of the saccade targets and the shifts in saccade endpoint.

For 199 targets from 21 experiments in monkey OZ we have plotted in Figure 2D the magnitude of the shift in saccade endpoint against the distance from each target to the injection site (t-inj). There was a minor trend for the magnitude of the

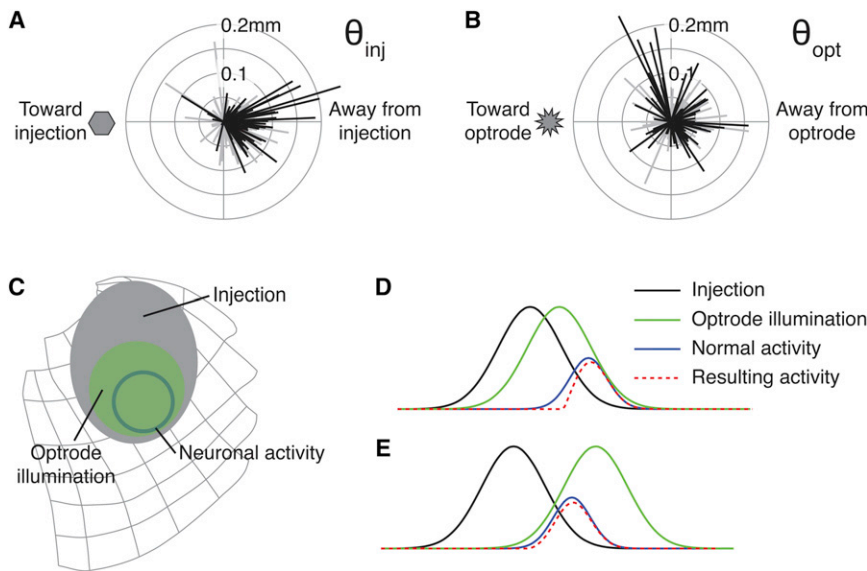


Figure 3. Saccades Are Deflected Away from the Injection, Not the Laser

(A) Shifts in saccade endpoints relative to the injection site for 199 separate targets from all experiments. (B) Shifts in saccade endpoints relative to the optrode site from all experiments. (C) Schematic of optogenetic influence of laser illumination on saccade-related neuronal activity in the SC. The gray ellipse is the proposed extent of the injection. The solid circle is the presumed population of neurons active during a saccade to a target about 12° to the right. The green superimposed on both shows the region supposedly illuminated by the laser. (D) Schematic of optogenetic influence in one dimension. The regions from (C) are now shown as Gaussian curves. When the laser (green curve) is positioned between the injection site (black curve) and the active neurons (blue curve), a subpopulation of neurons are inactivated, resulting in the neuronal activity represented by the dashed red curve, shifted away from the injection. (E) Distal placement of the laser still results in shifts away from the injection. See also Figure S2.

behavioral effect to reduce as t-inj increased ($r = -0.12$, $p = 0.12$). Figure 2E shows the same endpoint shifts as in Figure 2D, this time plotted against the distance on the SC from the target to the light (t-opt). Again the size of the behavioral effect was less for saccades more distant from the optrode. The black least-squares line to the data confirms this small trend ($r = -0.16$, $p = 0.02$). We must note, however, that there was a similar relationship between the shift in saccade endpoint and the magnitude of the saccade, t-ecc ($r = -0.11$, $p = 0.12$).

To determine the relative contributions of these three distances (t-inj, t-opt, t-ecc), we performed a multiple linear regression. These three factors sufficiently predicted the behavioral effect ($F = 3.7012$, $p = 0.0063$) although the distance from the target to the laser, t-opt, dominated the regression (coefficients: t-opt = -0.021 , $p = 0.002$; t-inj = -0.005 , $p = 0.320$; t-ecc = -0.001 , $p = 0.0254$).

In summary, the magnitude of the primary change in behavior we measured, the shift in saccade endpoint, was related to the proximity of both the injection site and the optrode site to the SC neurons underlying the saccade. However, these distances were not independent during an experiment, and further analysis showed that the magnitude of the saccadic shift was predominantly dependent on proximity to the laser illumination.

Relating the Direction of Shifts in Saccade Endpoint to Injection and Optrode Locations

Each shift in saccade endpoint was in a specific direction on the visual field map (Figure 2C). The next question was whether the directions of these shifts had any relation to either the location of the injection or the location of the laser light.

The first angle of interest θ_{inj} represents the direction of the mean shift in saccade endpoints relative to the injection site (see Figure S2). In short, if saccades shifted directly away from the injection site, θ_{inj} would be 0° (directly to the right in Figure 3A) whereas 180° (or -180°) would be directly toward the injection

site (directly to the left). We calculated θ_{inj} for saccades to each of the targets in each experiment. For 21 experiments in monkey OZ, Figure 3A shows the relative displacement vectors from the injection site for saccades to every target. Significant shifts are shown in black. Shifts in saccade endpoints were predominantly away from the injection site.

We performed this analysis again, this time measuring how saccade endpoints shifted away from the site of laser light, calculating the corresponding angle θ_{opt} . Figure 3B shows these shifts for all experiments. The pattern of shifts away from the laser is noticeably different than the shifts away from the injection site.

To summarize the selectivity of the directions of shifts we used a polar selectivity measure derived from the circular mean vector (Cavanaugh et al., 2002; Leventhal et al., 1995) in which we normalized the vector sum of the shifts by the sum of the shift magnitudes (see Supplemental Experimental Procedures). The angle of the resultant vector indicates the mean displacement direction. The magnitude of this vector is the degree of selectivity (0 for no selectivity to 1 for perfect selectivity). Significant deflections away from the injection site had a selectivity index of 0.765 at -10.5° (where 0° is directly away from the injection). Significant deflections away from the optrode had a selectivity index less than half that (0.37) at an angle of 31.4° . For all displacements, significant and nonsignificant, selectivity away from the injection site was 0.627 at -9.6° , whereas selectivity away from the optrode site was just 0.209 at 41.8° . In summary, these results demonstrate that saccades were more consistently and selectively deflected away from the injection site than away from the optrode site.

We believe this effect can be understood intuitively by considering three gradients: the gradient of the virally transfected neurons around the SC injection site, the gradient of light intensity around the optrode, and the gradient in the strength of neuronal activity with saccades made to a given target. These three regions are schematically illustrated on the map of the

SC in Figure 3C. The extents of the regions in this qualitative analysis are based on the areas we have observed in our experiments. We have taken these gradients into a single dimension in Figure 3D. Here each gradient is represented as a Gaussian curve. In this example, we have placed the optrode between the center of the injection and the saccade target. The dashed red curve shows the resultant neuronal activity according to a simple scheme; we multiplied the injection (transfected cells) by the illumination to represent the experimentally affected cells and subtracted this from the normal neuronal activation. When the laser is placed between the injection and the saccade target, neuronal activity is slightly shifted away from the injection, which would cause a small shift in saccades away from the injection site. In Figure 3E, the laser illumination has been placed on the other side of the target. The resulting neuronal activity is once again shifted slightly away from the injection, not the optrode, consistent with our observations. In net, we envision the effect of illumination on the gradient of transfected cells as being akin to shining a spotlight on a hillside. The light illuminates the slope of the hill, which defines the gradient of the shift in neuronal activity and the resulting shift in saccade endpoint.

Area of Neuronal Sensitization Measured by Neuronal Suppression

Behavioral changes give us some idea of the spatial spread of the optogenetic influence, but saccades are defined by the activity of a population of neurons that can span millimeters in the SC (1.4 mm estimated for SC burst cells; Munoz and Wurtz, 1995). Also, from Figure 2E, the laser illumination from the optrode could be affecting neurons over a millimeter away. A better estimate of the extent of sensitized neurons can be derived from the suppression of neuronal responses, the detection of which is limited to few hundred microns from the optrode. We pursued this in two monkeys, OZ and RO, making an effort to sample SC sites beyond the presumed center of the injection.

We used the established map of saccade directions and amplitudes across the intermediate layers of the SC to determine each optrode location, and characterized the degree to which we could affect neuronal responses with light at that location. We calculated the maximum reduction in response at each optrode site and produced a map by interpolating between the irregularly spaced data. Figure 4 shows the maps for the two monkeys. The area of the injection in OZ (Figure 4A) was clearly delineated at the lateral edge of the interpolated region where response differences diminished (whiter areas). We estimated the spread of the effect by fitting a two-dimensional Gaussian curve to the responses. The Gaussian was free to vary its center, orientation, height, and extent. We show the extent of the Gaussian (± 1 SD along each axis) as the dashed ellipse in Figure 4A. The region measured approximately 2,700 μm long by 2,100 μm across. For monkey RO (Figure 4B) the red ellipse indicates the actual extent of transfected neurons obtained from the histological evaluation described below.

Area of Neuronal Transfection Measured by Histological Reconstruction

Figure 4C shows how we constructed a three-dimensional representation of the injection in monkey RO from histological

sections. Our histological methods are explained in detail in Supplemental Experimental Procedures. For each of 11 coronal sections separated by 250 μm , we obtained the total number of neurons by counting the cells expressing the NeuN stain. We then counted which neurons expressed GFP, indicating transfection with the ArchT construct (see Figure S3). The marginal histograms in Figure 4C are simply the running means of the proportion of transfected cells in each section. Over the 11 sections, we used the extent of each running mean to establish the anterior-posterior and medial-lateral spread of the transfection. The central wireframe structure schematizes the three-dimensional reconstruction of the spread of the virus in monkey RO.

From our reconstruction, the injection extended approximately 2,500 μm along the anterior-posterior axis. The maximum extent of the injection along the medial-lateral axis was about 1,200 μm , and the extent along the dorsal-ventral axis was approximately 800 μm . The extent of this region can be seen on the collicular map of monkey RO in Figure 4B as the red dashed ellipse.

The injection shown in the histology was 6 μl (as opposed to 7 μl in monkey OZ). In addition, there is possible tissue shrinkage during processing. These factors may have contributed to the difference between injection spreads in Figures 4A and 4B. Since the tissue was sliced before staining, shrinkage does not apply to the AP dimension, which would contribute to the anisotropy of the injection in Figure 4B. Any residual anisotropy in either monkey could be due to a predominance of fibers in the intermediate layers running in the AP direction (Nakahara et al., 2006).

In summary, using the results from both the area of neuronal suppression within the SC (two monkeys) and the spread of GFP labeled neurons in the SC (one monkey), we estimate that single injection of 6–7 μl effectively sensitizes neurons to light in a region subtending about 2.5 mm by 2.3 mm horizontally.

DISCUSSION

What We Learn from Optogenetic Modulation of Saccadic Eye Movements

Neurons in the monkey have been shown previously to be activated or inactivated using optogenetic techniques (Diester et al., 2011; Han et al., 2009). We have now shown that monkey behavior also can be modified by optogenetic procedures, and described the conditions and parameters that govern success. Saccadic eye movements to visual targets showed the same trilogy of changes (a shift in saccadic endpoint, an increase in latency, and a decrease in velocity) with light-induced inactivation as with inactivation of SC by the anesthetic lidocaine or the GABA agonist muscimol.

These experiments show how the benefits of optogenetic tools translate to the study of primate behavior. First is the ability to have trials in which the target neurons are inactivated interleaved with those in which they are not. This permits comparison of experimental and control trials with only seconds of separation compared to chemical inactivation where control trials come long before or after the experimental trials. Second, there are minimal changes in optogenetic inactivation over a series of trials. In contrast, the effects of drug injections are always

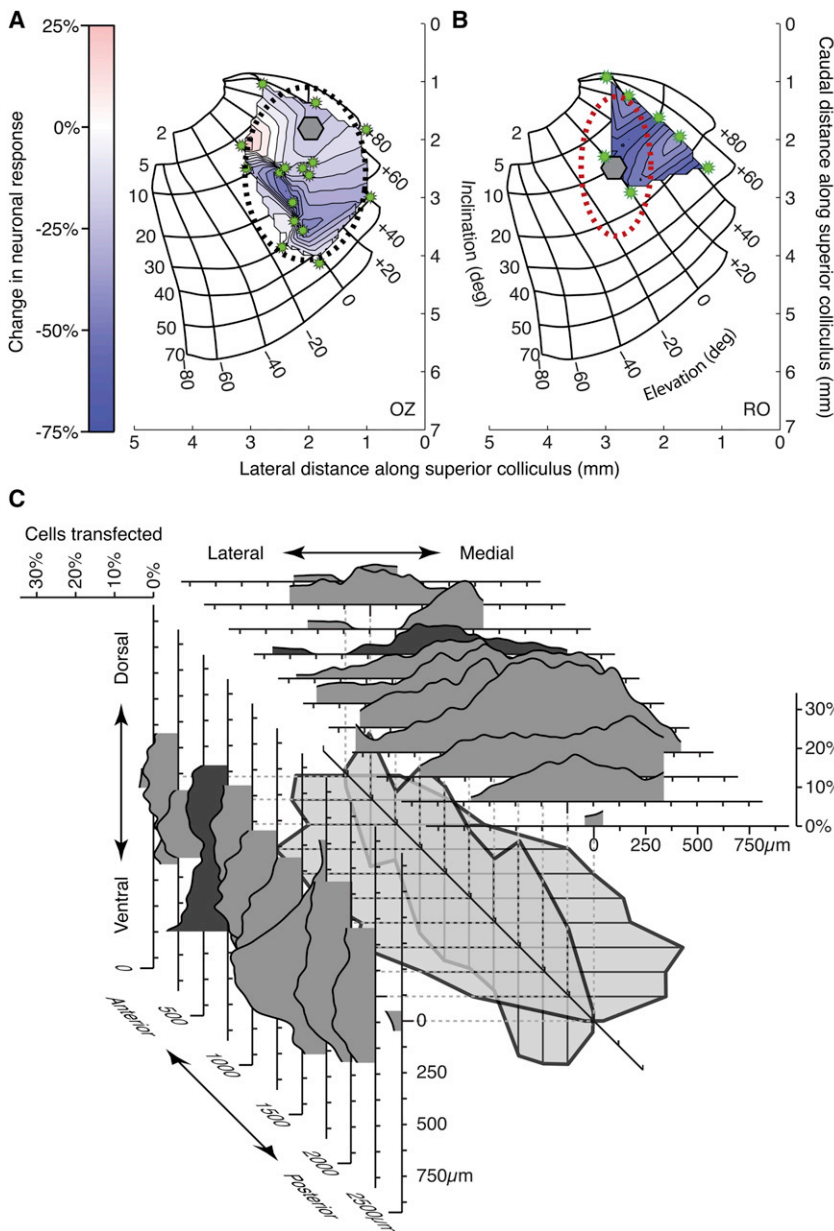


Figure 4. Spread of ArchT Transfection

The suppression of neuronal activity at several sites in the SC is shown for monkey OZ (A) and monkey RO (B). The injection site and optrode locations are shown as the hexagon and the starbursts, respectively. Axes indicate distance in mm along the SC. The color bar to the left shows how greater suppression is indicated by darker blue. Lighter regions in the interpolated area denote little change. The black ellipse shows the estimated extent of light sensitivity in monkey OZ determined by a 2D Gaussian fit to the data. The red ellipse in (B) shows the extent of the injection in Monkey RO determined from subsequent histological analysis. (C) For each of 11 histological sections from monkey RO we constructed marginal density plots (see [Supplemental Experimental Procedures](#)) representing the degree of transfection over the X and Y dimensions. Sections are aligned to the centers of their marginal distributions. The extents of transfection from each section have been combined in sequence in the center of the plot, with adjacent sections connected. This wireframe structure represents the spread of transfection in three dimensions. See also [Figure S3](#).

regions of inactivation, particularly when the relation of the area to behavior is tenuous. Small changes in behavior in such cases may go undetected, so a larger inactivation would probably be necessary to reveal the contribution of the structure to behavior. The limited size of the inactivation might well have contributed to the lack of any behavioral effect of channel rhodopsin injections made in monkey motor cortex ([Diester et al., 2011](#)).

Interaction of Static Injection Location and Movable Light Location

Optogenetic inactivation differs from chemical inactivation in having greater precision and added flexibility. With chemical inactivation, the effect on behavior is dependent on the overlap of the area of neurons active in generating the behavior (in our case a saccade) and the area of neurons inactivated by the chemical. With the optogenetic approach, however, there is a third gradient: the illumination from the optrode on targeted neurons. Essentially, the outcomes and interpretations of each optogenetic experiment are governed by the interaction of these three gradients.

The effect of these gradients on behavior was interesting: size of the effect depended on the saccade's distance from the optrode, and we would expect this factor to govern behavioral effects in any brain area. In addition, we found a systematic change in the direction of this shift that depended on the location of the injection. Saccade related neurons are mapped on the

changing due to the spread of the drug and its continual metabolizing. Third, techniques for injection and recording are similar to those already used in most laboratories studying the neuronal bases of behavior. Fourth, once the viral injection is made, localized inactivation can be shifted within the region of transfected neurons by simply moving the optrode, as is illustrated by [Figure 4](#). Finally, the area inactivated can be small enough to produce precise deficits such as those shown for the shifts in saccade endpoints in [Figure 3](#).

For other experiments, however, the small area of inactivation can be a substantial disadvantage. Saccade endpoints shifted on average about 5% of saccade magnitude, which for eye movements is readily measurable. In contrast, initial exploratory evaluation of a certain brain area frequently requires larger

intermediate layers of the SC as vectors pointing to different regions of the visual field. Activity during a saccade is the result of a large population of such neurons (Munoz and Wurtz, 1995), the average of whose vectors determines the generated saccade (Lee et al., 1988). In fact, the precision of the optogenetic method provides the most convincing evidence so far (Figure 3A) that shifts in saccade endpoints can be predicted if one knows the shift in the vector average resulting from inactivation. In our experiments, the shifts are most easily interpreted as the action of the injection gradient and the light gradient acting on the SC neuronal vector gradient, as indicated by the analysis in Figures 3C–3E.

Although chemical inactivation might well have a place in studying the brain, optogenetic techniques allow a new set of strategies with remarkable temporal and spatial precision, some of the principles of which we have illustrated here.

EXPERIMENTAL PROCEDURES

Three adult male monkeys (OZ, OM, RO; *Macaca mulatta*) provided data for different aspects of these experiments. Monkeys weighed between 8 and 11 kg and had implanted scleral search coils for measuring eye position, had recording cylinders for accessing SC neurons, and had posts for immobilizing the head during experiments as described previously (Sommer and Wurtz, 2000). All procedures were approved by the Institute Animal Care and Use Committee and complied with Public Health Service Policy on the humane care and use of laboratory animals.

Monkeys sat in a primate chair positioned 57 cm in front of a tangent screen. The chair was in a dark room in the center of magnetic field coils used for measuring eye movements. For monkeys OZ and OM, computers running REX (Hays et al., 1982) and associated programs controlled stimulus presentation, administration of reward, the recording of eye movements and single neuron activity, and the on-line display of results. For monkey RO, eye movements and neuronal data were acquired using a Plexon System. Visual stimuli appeared on a gray background on an LCD monitor or were back-projected by an LCD projector. Monkeys were rewarded with drops of fruit juice or water.

See Supplemental Experimental Procedures for further details.

SUPPLEMENTAL INFORMATION

Supplemental Information includes three figures and Supplemental Experimental Procedures and can be found with this article online at <http://dx.doi.org/10.1016/j.neuron.2012.10.016>.

ACKNOWLEDGMENTS

We are grateful to Altah Nichols and Tom Ruffner for machine shop support and to Kirk Thompson for his efforts in the initial stages of the experiments.

Accepted: October 17, 2012
Published: December 5, 2012

REFERENCES

- Cavanaugh, J.R., Bair, W., and Movshon, J.A. (2002). Selectivity and spatial distribution of signals from the receptive field surround in macaque V1 neurons. *J. Neurophysiol.* *88*, 2547–2556.
- Chow, B.Y., Han, X., Dobry, A.S., Qian, X., Chuong, A.S., Li, M., Henninger, M.A., Belfort, G.M., Lin, Y., Monahan, P.E., and Boyden, E.S. (2010). High-performance genetically targetable optical neural silencing by light-driven proton pumps. *Nature* *463*, 98–102.
- Diester, I., Kaufman, M.T., Mogri, M., Pashaie, R., Goo, W., Yizhar, O., Ramakrishnan, C., Deisseroth, K., and Shenoy, K.V. (2011). An optogenetic toolbox designed for primates. *Nat. Neurosci.* *14*, 387–397.
- Han, X., Qian, X., Bernstein, J.G., Zhou, H.H., Franzesi, G.T., Stern, P., Bronson, R.T., Graybiel, A.M., Desimone, R., and Boyden, E.S. (2009). Millisecond-timescale optical control of neural dynamics in the nonhuman primate brain. *Neuron* *62*, 191–198.
- Han, X., Chow, B.Y., Zhou, H., Klapoetke, N.C., Chuong, A., Rajimehr, R., Yang, A., Baratta, M.V., Winkle, J., Desimone, R., and Boyden, E.S. (2011). A high-light sensitivity optical neural silencer: development and application to optogenetic control of non-human primate cortex. *Front. Syst. Neurosci.* *5*, 18.
- Hays, A.V., Richmond, B.J., and Optican, L.M. (1982). A UNIX-based multiple process system for real-time data acquisition and control. *WESCON Conference Proceedings 2*, 1–10.
- Hikosaka, O., and Wurtz, R.H. (1985). Modification of saccadic eye movements by GABA-related substances. I. Effect of muscimol and bicuculline in monkey superior colliculus. *J. Neurophysiol.* *53*, 266–291.
- Hikosaka, O., and Wurtz, R.H. (1986). Saccadic eye movements following injection of lidocaine into the superior colliculus. *Exp. Brain Res.* *61*, 531–539.
- Knöpfel, T., and Boyden, E.S. (2012). Tools for observing and controlling specific molecular or physiological pathways in intact cells and tissues. Preface. *Prog. Brain Res.* *196*, vii–viii.
- Lee, C., Rohrer, W.H., and Sparks, D.L. (1988). Population coding of saccadic eye movements by neurons in the superior colliculus. *Nature* *332*, 357–360.
- Leventhal, A.G., Thompson, K.G., Liu, D., Zhou, Y., and Ault, S.J. (1995). Concomitant sensitivity to orientation, direction, and color of cells in layers 2, 3, and 4 of monkey striate cortex. *J. Neurosci.* *15*, 1808–1818.
- Munoz, D.P., and Wurtz, R.H. (1995). Saccade-related activity in monkey superior colliculus. II. Spread of activity during saccades. *J. Neurophysiol.* *73*, 2334–2348.
- Nakahara, H., Morita, K., Wurtz, R.H., and Optican, L.M. (2006). Saccade-related spread of activity across superior colliculus may arise from asymmetry of internal connections. *J. Neurophysiol.* *96*, 765–774.
- Robinson, D.A. (1972). Eye movements evoked by collicular stimulation in the alert monkey. *Vision Res.* *12*, 1795–1808.
- Sommer, M.A., and Wurtz, R.H. (2000). Composition and topographic organization of signals sent from the frontal eye field to the superior colliculus. *J. Neurophysiol.* *83*, 1979–2001.
- Tye, K.M., and Deisseroth, K. (2012). Optogenetic investigation of neural circuits underlying brain disease in animal models. *Nat. Rev. Neurosci.* *13*, 251–266.